Multi-layer asymptotic solution for wetting fronts in porous media with exponential moisture diffusivity

By Christopher J. Budd and John M. Stockie

We study the asymptotic behaviour of sharp front solutions arising from the nonlinear diffusion equation $\theta_t = (D(\theta)\theta_x)_x$, where the diffusivity is an exponential function $D(\theta) = D_o \exp(\beta\theta)$. This problem arises for example in the study of unsaturated flow in porous media where θ represents the liquid saturation. For physical parameters corresponding to actual porous media, the diffusivity at the residual saturation is $D(0) = D_o \ll 1$ so that the diffusion problem is nearly degenerate. Such problems are characterised by wetting fronts that sharply delineate regions of saturated and unsaturated flow, and that propagate with a well-defined speed. Using matched asymptotic expansions in the limit of large β, we derive an analytical description of the solution that is uniformly valid throughout the wetting front. This is in contrast with most other related analyses that instead truncate the solution at some specific wetting front location, which is then calculated as part of the solution, and beyond that location the solution is undefined. Our asymptotic analysis demonstrates that the solution has a four-layer structure, and by matching through the adjacent layers we obtain an estimate of the wetting front location in terms of the material parameters describing the porous medium. Using numerical simulations of the original nonlinear diffusion equation, we demonstrate that the first few terms in our series solution provide approximations of physical quantities such as wetting front location and speed of propagation that are more accurate (over a wide range of admissible β values) than other asymptotic approximations reported in the literature.

1. Introduction

Problems with exponential diffusivity arise commonly in the study of water transport in variably-saturated porous media such as soil, rock or building materials [1]. An example of such, expressed in dimensionless form, is the one-dimensional nonlinear diffusion problem

$$\frac{\partial\theta}{\partial t} = \frac{\partial}{\partial x}\left(D(\theta)\frac{\partial\theta}{\partial x}\right), \tag{1a}$$

$$\theta(0,t) = \theta_i \quad \text{and} \quad \theta(L,t) = \theta_o \quad \text{for } t \geqslant 0, \tag{1b}$$

$$\theta(x,0) = \theta_o \quad \text{for } 0 < x < L, \tag{1c}$$

where the solution $\theta(x,t)$ is called *saturation* and represents the volume fraction of pore space occupied by liquid. We are concerned here with the case when the dimensionless variable $L \gg 1$

Address for correspondence: John M. Stockie, Department of Mathematics, Simon Fraser University, 8888 University Drive, Burnaby, BC, V5A 1S6, Canada; email: stockie@math.sfu.ca

DOI: 10.1146/((please add article doi))
Stud. Appl. Math. AA:1–28

and the diffusivity is an *exponential function* of the solution having the form

$$D(\theta) = D_o e^{\beta\theta}, \tag{1d}$$

where D_o and β are constants satisfying $0 < D_o \ll 1$ and $\beta \gg 1$. This is a reasonable model for horizontal infiltration problems such as that pictured in Figure 1a, where liquid is taken up by capillary action within a dry porous medium and gravity can be neglected. Many experimental studies of porous media have been performed in which an exponential diffusion ansatz provides a good fit with measured data, mostly in the context of water transport in soil and rock [1, 2, 3, 4], but also for other porous materials such as wood [5], brick [6] or concrete [7]. Exponential diffusion has also been identified in other transport phenomena as diverse as heat conduction [8], optical lithography [9], solvent transport in polymers [10], and diffusion of impurities in oxides [11]. The significance of this type of diffusion coefficient is that if $\theta_i > \theta_o$ and if β is even moderately large then $D(\theta)$ varies rapidly with θ, thereby causing solutions of (1a) to develop a steep interface, called a *wetting front* in the context of porous media flow, that is associated with localised high curvature and an exponential change in the solution gradient (see Figure 1b). The aim of this paper is to perform an asymptotic analysis of this phenomenon and in particular to study self-similar solutions of (1a) using a multi-layer asymptotic expansion, supported by numerical calculations. The asymptotic theory is especially subtle owing to the exponential change in the solution gradient and yields sharp estimates that agree well with numerical simulations.

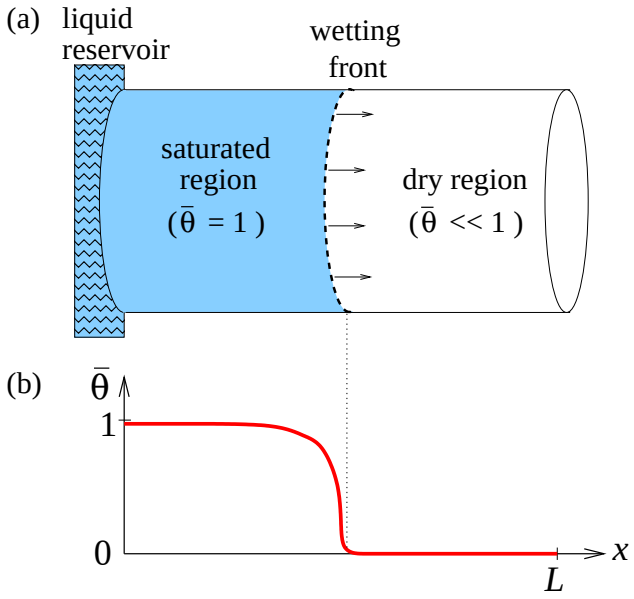

Figure 1. (a) A cylindrical porous medium with the left end immersed in a water reservoir, depicting the progress of a wetting front to the right owing to capillary action. (b) Plot of rescaled saturation $\bar{\theta} = (\theta - \theta_o)/(\theta_i - \theta_o)$ along the length of the cylinder from $x = 0$ to L.

1.1. Overview of Previous Work

The nonlinear diffusion equation (1a) has been studied in considerable detail for diffusivities $D(\theta)$ having a variety of functional forms. Particular emphasis has been placed on the special case of

a power law, $D(\theta) = D_o\theta^m$ with $m > 0$, for which (1a) is called the *porous medium equation* or PME; an extensive literature exists for the PME that is thoroughly covered in the review by Vázquez [12]. In a typical wetting scenario the PME is supplemented by boundary conditions $\theta(0,t) = 1$ and $\theta(\infty,t) = 0$, in which case the solution for a power-law diffusivity is well known to have compact support and to consist of a front propagating to the right with speed proportional to $t^{-1/2}$. Ahead of the front, the solution is identically zero and when $m \geqslant 1$ there is a discontinuity in the first derivative θ_x at the point where the front meets the x-axis; otherwise, when $0 < m < 1$, the wetting front meets the leading edge solution smoothly. The trailing edge of the front, on the other hand, always experiences a smooth transition similar to that shown in the saturation profile in Figure 1b. Analytical results have been derived for other types of diffusion coefficient, for example by Shampine [13] who provides an existence-uniqueness proof for a general class of diffusivity functions with $D(\theta)$ required to be a continuously differentiable function on $0 \leqslant \theta \leqslant 1$, satisfying $D(0) = 0$ and $D(\theta) > 0$ when $\theta > 0$. This and other analytical studies are characterised by the fact that they pertain to *degenerate diffusion* for which the diffusivity vanishes identically at zero saturation.

In contrast with this previous work, the diffusion coefficient we consider in this paper is an exponential function of saturation that, although small, is still bounded away from zero; hence the solution remains everywhere classical and all disturbances propagate with infinite speed, analogous to solutions of the "usual" heat equation. When the PME wetting scenario described above is repeated for an exponential diffusivity, the solution remains non-zero for all times $t > 0$, even when the initial conditions have bounded support. Nonetheless, the problem can be *nearly degenerate* in the sense that $D(0) \ll 1$ whereas $D(\theta) = \mathcal{O}(1)$ for θ away from zero. For example, typical parameter values for a porous soil have been estimated as $D_o \approx 2\times10^{-9}\ m^2/s$ and $\beta \approx 20$ [4]. For such diffusion coefficients, the solution inherits features that are qualitatively similar to the degenerate problem, most notably a steep wetting front that propagates with finite speed and that is associated with localised high curvature (see Figure 2(b)). We define the wetting front location $x_*(t)$ to be the point where the curvature of $\theta(x,t)$ is greatest, and for $x > x_*$ we have that $\theta_x \ll 1$. One feature that distinguishes the exponential diffusion equation from the PME is the fact that θ exhibits more rapid variation than for a power law, which in turn has a substantial impact on the shape of the solution close to the wetting front. A direct comparison is afforded by Leech et al.'s study of concrete [7] wherein they use experimental data to fit both power-law and exponential diffusivities, yielding respectively $D(\theta) = D_o\theta^4$ and $D(\theta) = D_o e^{6\theta}$. In Figure 2, we plot the diffusion coefficients and corresponding saturation profiles for these two choices of $D(\theta)$. While the qualitative features of both solutions are similar, there is a significant difference in both the steepness and location of the wetting front, as well as the sharpness of the corner (refer to the zoomed-in region in Figure 2(b)). Another distinguishing feature is that the solution in the exponential case is characterized by a small nonzero saturation ahead of the wetting front due to the fact that $D(0) \neq 0$.

Following up on these experimental studies, several authors have derived theoretical results for the exponential diffusion problem. Crank's book [14] provides a comprehensive treatment of analytical solutions for nonlinear diffusion equations circa 1975 with many forms of the diffusivity function. In particular, Crank derives a similarity solution for the exponential diffusion case (following the work of Cooper [8]) that reduces the problem to a second-order ordinary differential equation (ODE) which he then solves numerically – indeed, this is the same ODE that we will present later in Section 3. An alternate approach using functional iteration has been developed based on an integral formulation of the governing equations by Parslow et al. [15].

In contrast with these iterative or numerical solution methods, we are interested here in developing an asymptotic series representation of the solution. One study of particular relevance is

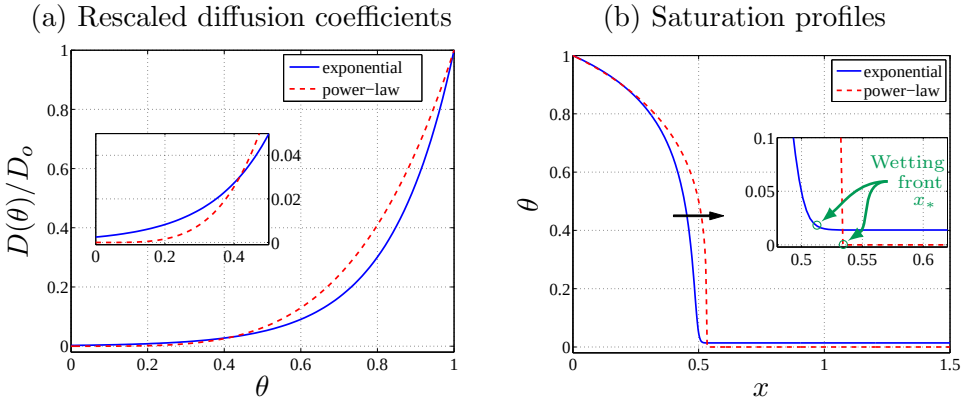

Figure 2. Comparison of solutions to the nonlinear diffusion problem for both power-law and exponential diffusion coefficients, $D(\theta) = D_o\theta^4$ and $D(\theta) = D_o e^{6\theta}$. (a) On the left is the rescaled diffusivity $D(\theta)/D_o$. (b) On the right are the corresponding saturation profiles $\theta(x,t)$ computed numerically at some fixed time $t > 0$. The black arrow indicates the direction of the wetting front motion, from left to right. The green arrows within the inset plot denote the wetting front x_* for each solution, located at the point of maximum curvature.

due to Babu [16] who derived an asymptotic solution by making use of the simplifying assumption that both saturation and diffusivity drop to zero ahead of a certain wetting front location. Although Babu's asymptotic estimates are reasonably accurate, we will demonstrate that his approach of truncating the solution at the wetting front introduces significant errors that can be reduced by considering an alternate approach that incorporates the effect of the extremely small but still nonzero diffusivity values ahead of the front. Other alternate series expansions based on an integral form of the exponential diffusion equation were derived by Parlange and co-workers in [17, 18]. Finally, we point out a connection to the work of Elliott et al. [19] who applied methods from singular perturbation theory to analyse the detailed structure of the transition region for the power-law diffusivity $D(\theta) = D_o\theta^m$ in the limiting case of $m \to \infty$, which is known as the *mesa problem*. Although this problem is still degenerate, the diffusivity in the large-m limit experiences a rate of increase in θ approaching that of an exponential function; therefore, the analysis for the mesa problem can be considered as a prototype for problems such as (1). Asymptotic solutions were developed for a semi-conductor dopant diffusion problem by King [20] for the two limits $m \to 0$ (constant D) and $m \to \infty$ (mesa), and King and Please [21] applied singular perturbation theory to obtain a matched asymptotic solution for the case $m = 1$ (linear D); however, the asymptotic structure of the solution for the exponential diffusion problem has not yet been explored in similar detail.

1.2. Summary of Main Results

We will demonstrate in this paper that a multi-layer asymptotic expansion is capable of yielding an accurate estimate of the wetting front location, provided that the exponentially varying solution is properly resolved close to the front. In particular, we will show that there is a self-similar solution $\Theta(y)$ that can be written in terms of the dimensionless similarity variable

$$y = \frac{x}{\sqrt{2tD(\theta_i)}}.$$

The corresponding wetting front location y_* is a constant and has the asymptotic expansion

$$y_* = \frac{1}{\gamma} + \frac{1}{2\gamma^3} + \frac{11}{12\gamma^5} + \mathcal{O}\left(\frac{1}{\gamma^7}\right).$$

The large parameter $\gamma = -\Theta'(0)$ is related to the physical constant β through the asymptotic expression

$$\bar{\beta} \equiv \beta\left(\theta_i - \theta_o\right) = \gamma^2 + \frac{1}{2} + \frac{\alpha_3}{\gamma^2} + \mathcal{O}\left(\frac{1}{\gamma^4}\right) \gg 1,$$

where $\alpha_3 \approx \frac{1}{12}$ is obtained numerically. Our asymptotic solution is distinct from other approximations derived in the literature in that it provides insight into the detailed structure of the wetting front, as well as yielding estimates of quantities such as y_* that are accurate over a wide range of parameters. The estimate of wetting front location could be of particular interest to engineers since it expresses an easily measurable quantity in terms of physical parameters.

The remainder of this paper is structured as follows. In Section 2 we motivate the problem under study by using the example of water transport in unsaturated porous media, although we stress that these results are equally applicable to other nonlinear diffusion problems having an exponential diffusivity. In Section 3 we introduce a similarity transformation that permits us to recast problem as an ODE initial value problem, for which $\gamma \gg 1$ is related to the magnitude of the initial slope of the similarity solution. Section 4 derives our key results, consisting of a four-layer asymptotic expansion for the similarity solution, expressed as a series in γ on each layer. Matching the asymptotic expressions then yields series approximations for the quantities of physical interest such as the saturation and curvature at the sharp corner in the wetting front, as well as the location x_* of the front itself. In Section 6 we perform a detailed comparison of our asymptotic solution to other approximations in the literature, as well as validating the results with careful numerical simulations of the original governing partial differential equation.

2. Physical Background

Water transport in a saturated porous medium is well-known to obey Darcy's law [22], $\boldsymbol{U} = -K\nabla\Phi$, which states simply that the liquid velocity $\boldsymbol{U}$ (in m/s) is proportional to the gradient of total hydraulic potential Φ (in m). The proportionality constant K is known as the hydraulic conductivity and has units of m/s. However, many porous media flows are unsaturated, which means that the pore volume is only partially filled with liquid, and in this case it is necessary to introduce the liquid volume fraction or saturation, θ. The conductivity in a variably saturated porous medium is typically assumed to depend on the local saturation, leading to an extended Darcy's law, $\boldsymbol{U} = -K(\theta)\,\nabla\Phi$, that includes a saturation-dependence in the hydraulic conductivity. When this expression for velocity is substituted into the continuity equation

$$\frac{\partial\theta}{\partial t} + \nabla\cdot\boldsymbol{U} = 0,$$

we obtain an evolution equation for θ

$$\frac{\partial\theta}{\partial t} = \nabla\cdot\left(K(\theta)\nabla\Phi\right), \tag{2}$$

which is known as the *Richards equation*. If both Φ and K are assumed to be single-valued functions of saturation, then we can define $D(\theta) := K(\theta)\left(d\Phi/d\theta\right)$ after which Eq. (2) reduces to the familiar

nonlinear diffusion equation

$$\frac{\partial \theta}{\partial t} = \nabla \cdot (D(\theta)\nabla\theta)\,,$$

for which Eq. (1a) is the 1D version. The function $D(\theta)$ is referred to as the *moisture diffusivity* and has units of m^2/s. As mentioned in the Introduction, the exponential form (1d) for diffusivity is motivated by the study of certain soils and porous building materials, for which an exponential function provides a good fit to experimental data.

We consider an idealised, cylindrical geometry depicted in Figure 1a that is consistent with the samples typically used in experimental studies of moisture transport. The porous cylinder is initially dry and has one end placed in a water reservoir. We are interested in problems such as the *horizontal infiltration* scenario pictured, or where capillary forces dominate over gravity, so that water is absorbed into the porous medium by capillary action alone. Water progresses into the sample as a nearly planar wetting front, and so we can assume that the flow is uni-directional and governed by the one-dimensional diffusion equation (1a). The length of the sample is denoted by L, which is presumed large in relation to the diameter so that $L \gg 1$.

In order to treat a general class of wetting scenarios we take samples that are never completely dry, which corresponds to the usual situation wherein a porous medium undergoes re-wetting after an initial wetting/draining cycle. Consequently, there exists a non-zero minimum or residual saturation $\theta = \theta_o$ deriving from water that is trapped in isolated portions of the porous matrix and which cannot be displaced by capillary action. Furthermore, we introduce a maximum saturation $\theta_i \leqslant 1$ that cannot be exceeded owing to micropores that are too small to allow water to penetrate, no matter how large the capillary force. Consequently, the saturation θ satisfies $0 < \theta_o \leqslant \theta \leqslant \theta_i \leqslant 1$, while the boundary and initial conditions are as specified in (1b) and (1c). Water content is usually reported in the literature in terms of *reduced saturation*

$$\bar{\theta} = \frac{\theta - \theta_o}{\theta_i - \theta_o} = \frac{\theta - \theta_o}{\Delta\theta},$$

for which the boundary and initial conditions reduce to

$$\bar{\theta}(0,t) = 1, \qquad \bar{\theta}(L,t) = 0 \quad \text{and} \quad \bar{\theta}(x,0) = 0. \tag{3}$$

A picture of a typical wetting front is displayed in Figure 1b in terms of the rescaled saturation variable $\bar{\theta}$.

3. Self-Similar Solution

We are now interested in finding a self-similar solution of the nonlinear diffusion equation on the half-space $x \in [0,\infty]$, when $L \to \infty$, and which satisfies the Dirichlet boundary condition $\theta(0,t) = \theta_o$ constant. The problem (1) is invariant under the scaling transformation $y = xt^{-1/2}$, which suggests seeking a solution of the form $\theta(x,t) = \phi(y)$, where the specific form of the similarity variable

$$y = \frac{x}{\sqrt{2tD(\theta_i)}} \tag{4}$$

is chosen to eliminate certain constants from the ODE and boundary conditions. We then define the new dependent variable

$$\Theta := e^{\beta(\phi(y)-\theta_i)} \qquad \text{or equivalently} \qquad \Theta := e^{\bar{\beta}(\bar{\theta}-1)}, \tag{5}$$

where

$$\bar{\beta} := \beta\Delta\theta = \beta(\theta_i - \theta_o).$$

This form of solution is consistent with the second boundary condition (1b) provided that $L/\sqrt{D(\theta_i)t} \gg 1$, which motivates our taking $L \to \infty$ in what follows. This simplifies the problem further by eliminating the exponential diffusion coefficient (1d), leading to the following ODE boundary value problem for $\Theta(y)$:

$$\Theta\Theta'' = -y\Theta' \qquad \text{for } 0 < y < \infty, \tag{6a}$$

$$\Theta(0) = 1, \tag{6b}$$

$$\Theta(\infty) = \Theta_\infty := e^{-\bar{\beta}}. \tag{6c}$$

For the porous media of interest here, $\bar{\beta}$ is significantly greater than one so that the parameter Θ_∞ satisfies $0 < \Theta_\infty \ll 1$.

Rather than solving Eqs. (6) directly it is convenient, for both the numerical and the asymptotic calculations, to reformulate this boundary value problem as an initial value problem, in which the boundary condition (6c) is replaced by a second initial condition of Neumann type given by

$$\Theta'(0) \ = \beta\phi'(0) = -\gamma, \tag{6c$'$}$$

where $-\gamma$ represents the initial slope which we will assume to be large. From this point on, we use (6′) to refer to the initial value problem consisting of equations (6a), (6b) and (6c′). The asymptotic analysis performed in this paper considers the limit of $\gamma \to \infty$ which we will see shortly is equivalent to taking $\Theta_\infty \to 0$. The quantity γ is not known *a priori* in terms of the physical parameters, and so one of the primary results of this paper will be to first derive asymptotic expressions for $\bar{\beta}$ and y_* in terms of γ and to then invert them to give γ in terms of the physical quantities.

Before moving on, we address the suitability of applying alternate boundary conditions of Neumann (or flux) type. First of all, it follows from equations (6a) and (6b), along with a later result indicating $\Theta''(\infty) \sim 0$, that the Dirichlet problem above has an implicit no-flux (zero Neumann) condition at infinity. Hence, there is no need to consider this case separately. When the left boundary condition is replaced with a flux contition of the form $\theta_x(0,t) = a$, no similarity solution is permitted unless $a = 0$, and in the zero-flux case there is only the trivial solution $\Theta \equiv \Theta_\infty$. Therefore, it is sufficient to focus on the Dirichlet problem in (6).

3.1. Preliminary Numerical Simulations

Before proceeding with the analysis, we present several plots that illustrate the asymptotic behaviour of the self-similar solution for large γ, computed via numerical simulations of the initial value problem (6′). We use a shooting algorithm wherein a value of $\bar{\beta}$ is chosen, and then $\gamma = -\Theta'(0)$ is updated iteratively until Θ is sufficiently close to the right hand boundary value $\Theta_\infty = e^{-\bar{\beta}}$. This approach is similar to that employed by others for the exponential diffusion problem [14, 23], and more details on our shooting algorithm are given in Section 6.1. For illustration purposes, we choose physical parameters corresponding to a typical soil water uptake experiment [4]. Taking limiting values of $\theta_o = 0.04$ and $\theta_i = 0.43$, and an unsaturated diffusivity $\beta = 20.5$, we obtain parameters $\Delta\theta = 0.39$, $\bar{\beta} = 8.0$ and $\Theta_\infty = \exp(-8.0) = 3.4 \times 10^{-4}$, which clearly satisfies the requirement $\Theta_\infty \ll 1$. We remark that other experiments on water transport in a wide range of porous media (including soils, concrete, and other building materials) suggest that allowable values of $\bar{\beta}$ are restricted to a fairly narrow interval of $4 \lessapprox \bar{\beta} \lessapprox 9$. The resulting numerical solution is depicted in the two rightmost plots in Figure 3(c). The upper plot displays the computed similarity

solution $\Theta(y)$ while the lower plot shows the corresponding curves for reduced saturation $\bar{\theta}(x,t)$ at ten equally-spaced time intervals, which are determined from $\Theta(y)$ by transforming back to physical variables Eq. (4).

The computed solution for $\bar{\beta} = 8$ exhibits a well-defined wetting front that manifests in the $\bar{\theta}$ plot as a narrow region with a steep slope located immediately behind a sharp corner. In the plot of Θ on the other hand, the steep front has been eliminated by the exponential stretching transformation (5), but the wetting front location is still identified with a sharp corner. A zoomed-in view of the wetting front is shown in the inset for $\bar{\beta} = 8$ and clearly indicates that the solution within the corner region transitions rapidly to a small value of saturation, but this transition remains smooth.

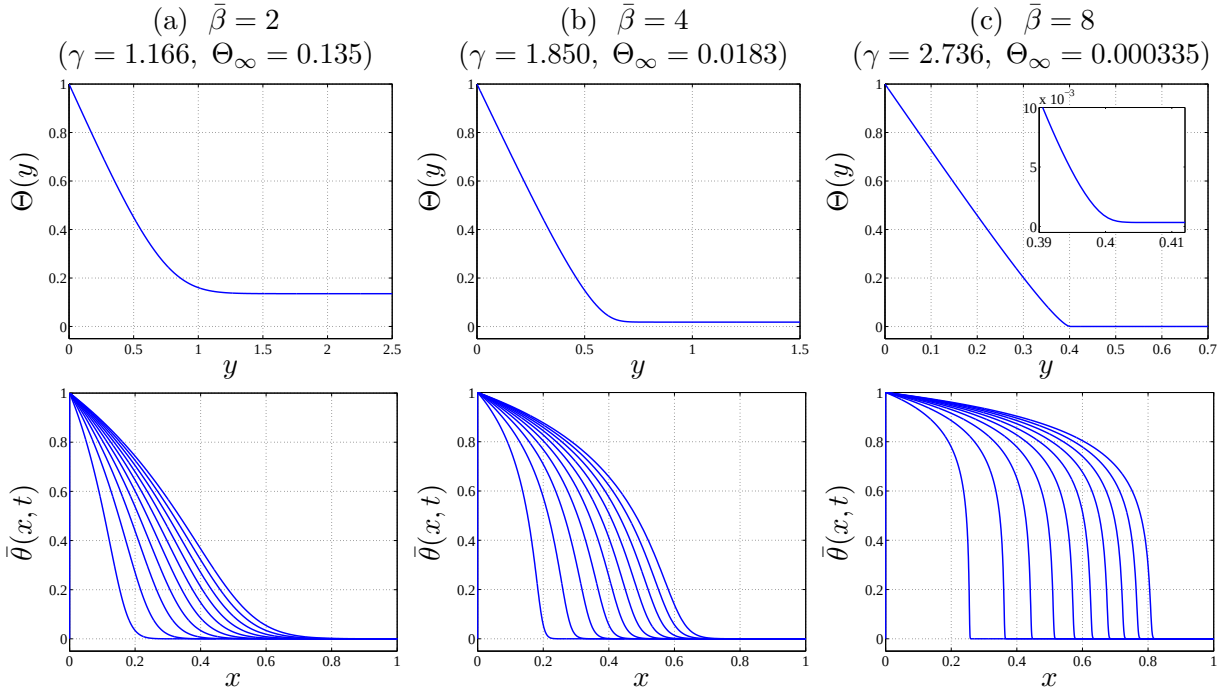

Figure 3. Saturation for values of $\bar{\beta} = \beta\Delta\theta = 2$ (left), 4 (middle) and 8 (right). The top row shows the similarity variable $\Theta(y)$ obtained by solving Eqs. (6′) numerically. The bottom row contains corresponding plots of the reduced saturation, $\bar{\theta}(x,t) = 1 + (\log\Theta)/\bar{\beta}$, with time t taken at ten equally-spaced points. The inset at the top right is a zoomed-in view of the sharp corner.

Additional pairs of solution plots are given in Figures 3(a,left) and 3(b,middle) for values of $\bar{\beta} = 2$ and 4 respectively. Clearly, taking $\bar{\beta}$ smaller (or equivalently Θ_∞ larger) causes the wetting front to exhibit a more gradual slope and a milder transition through the corner region, and in the extreme case of $\bar{\beta} = 2$ there is hardly any evidence of a wetting front at all. However, as we have indicated above, most problems of physical interest correspond to values of $\bar{\beta} \geqslant 4$ and this observation has an important effect on the accuracy of our asymptotic solution derived in Section 4.

We next investigate in more detail the effect on the similarity solution $\Theta(y)$ of changes in $\bar{\beta}$. In particular, Figure 3 indicates that as $\bar{\beta}$ increases the value of γ likewise increases, which leads to a steeper initial slope and a corresponding shift of the wetting front location toward the origin along the y–axis. A number of additional simulations are performed for γ lying in the interval $[0.5, 5.0]$ and the corresponding values of $\bar{\beta}$ are plotted in Figure 4(a). By performing a least-squares polynomial

fit to the computed points, we obtain to a very good approximation the quadratic polynomial fit

$$\bar{\beta} = -\log \Theta_\infty \approx \gamma^2 + \frac{1}{2},$$

which when displayed in Figure 4(a) alongside the computed data is nearly indistinguishable. This relationship between $\bar{\beta}$ and γ will be verified later in Section 4 when it is derived as part of our asymptotic solution.

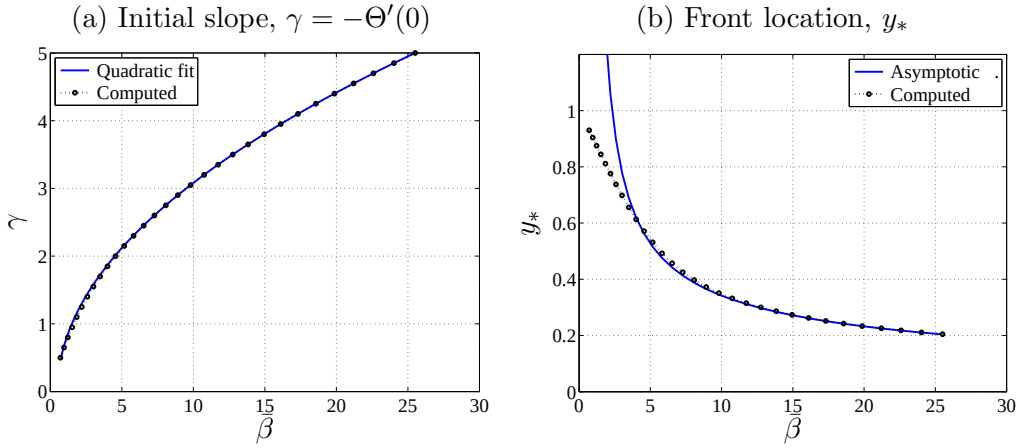

Figure 4. Left: Values of $\bar{\beta}$ and $\gamma = -\Theta'(0)$ obtained from numerical simulations of Eq. (6′) with parameters chosen as in Figure 3. The quadratic fit $\bar{\beta} = \gamma^2 + 1/2$ is shown as a solid line for comparison purposes. Right: The computed wetting front location (estimated using the point of maximum curvature) is depicted along with the two-term asymptotic approximation from Eq. (15).

It is evident from the plots in Figure 3 that for $\bar{\beta}$ sufficiently large there exists a sharp corner in the similarity solution $\Theta(y)$ that can be identified with the wetting front location in plots of saturation $\bar{\theta}$. In contrast with the power-law diffusion problem, where the wetting front is identified with a discontinuity in the solution derivative, the exponential diffusion problem exhibits a smooth transition through the front and so there is no unique front position. We therefore choose to identify the wetting front location y_* with the point of maximum curvature in Θ which satisfies $\Theta''(y_*) = 0$. We provide a preview of our asymptotic results in Figure 4(b), which depicts the computed front location y_* as a function of $\bar{\beta}$, alongside our our two-term asymptotic approximation of y_* derived later in Section 4.2. Clearly, the analytical results are quite accurate for $\bar{\beta}$ in the physical range.

4. Multi-Layer Asymptotic Solution

4.1. Overview

In this section, we will derive the asymptotic form of the solution for large γ. The preliminary numerical results already shown in Figure 3 suggest that the solution for large $\bar{\beta}$ (and hence large γ) can be separated into four regions or layers:

(a) An linear *inner solution* in which $\Theta(y)$ is close to linear and has gradient close to $1/\gamma$. This region extends over a range of y values lying between 0 and slightly below $1/\gamma$ where the solution is determined by the initial conditions at $y = 0$.

(b) A nearly constant *outer solution* on the right of y_*, where the solution is determined by the far field condition as $y \to \infty$. Here the solution approaches Θ_∞ for y sufficiently large (in fact, for y only a little greater than y_*).

(c) An *intermediate-range solution* containing the wetting front at y_* and of width $\Delta y = \mathcal{O}(1/\gamma^3)$. In this region we see the rapid transition through the corner of the wetting front and the solution has (locally) and exponentially (in γ) large curvature. In the intermediate range, we see a transition from the linear solution, which is of order $1/\gamma^2$ when $y = 1/\gamma$, to one exponentially small in γ for $y > y_* = 1/\gamma + 1/2\gamma^3 + \mathcal{O}\left(1/\gamma^5\right)$. It will prove convenient to divide this intermediate layer into a *left-range* and a *right-range* to capture this behaviour to high order.

These regions are depicted schematically in Figure 5 in terms of the similarity variable $\Theta(y)$. We expect that our asymptotic approximation will be inaccurate for small values of $\bar{\beta}$ when the inner solution is more curved behind the front, but will improve as $\bar{\beta}$ increases and the inner solution becomes closer to linear.

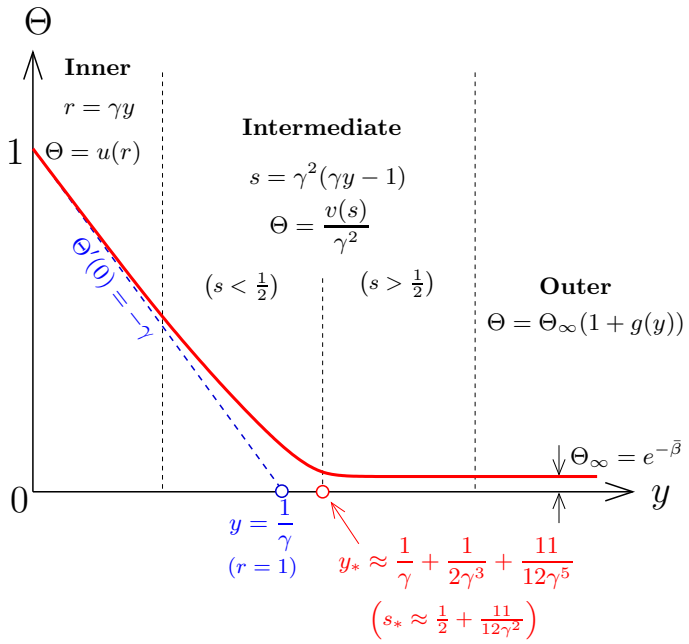

Figure 5. The similarity solution $\Theta(y)$ is separated into several regions: an inner region on the left consisting of a nearly linear solution $u(r)$; an outer region on the right where the solution is nearly constant; and an intermediate region near the wetting front $y = y_*$ within which an intermediate-range solution of locally high curvature connects the inner and outer solutions.

Before going into the details, we first summarise the main result for the wetting front location

$$y_* = \frac{1}{\gamma} + \frac{1}{2\gamma^3} + \frac{11}{12\gamma^5} + \mathcal{O}\left(\frac{1}{\gamma^7}\right). \tag{7}$$

By taking y_* as the point of maximum curvature in saturation $\Theta(y)$, we may then approximate the values of both saturation and curvature at the wetting front by

$$\Theta(y_*) \approx e\Theta_\infty \quad \text{and} \quad \Theta''(y_*) \approx \frac{1}{\gamma^2} e^{\gamma^2 - 1/2}. \tag{8}$$

We will show further that

$$\Theta\left(\frac{1}{\gamma}\right) = \frac{1}{2\gamma^2} + \frac{b - \log(\gamma)}{\gamma^4} + \mathcal{O}\left(\frac{1}{\gamma^6}\right) \quad \text{where} \quad b = \frac{11}{12} - \frac{1}{2}\log 2. \tag{9}$$

Finally, the physical parameter $\bar{\beta}$ can be expressed as

$$\bar{\beta} = -\log \Theta_\infty = \gamma^2 + \frac{1}{2} + \frac{\alpha_3}{\gamma^2} + \mathcal{O}\left(\frac{1}{\gamma^4}\right), \tag{10}$$

where α_3 is a constant that we can estimate numerically as $\alpha_3 = 1/12$. It follows immediately that for large $\bar{\beta}$ we have

$$\gamma = \bar{\beta}^{1/2} - \frac{1}{4}\bar{\beta}^{-1/2} - \left(\frac{\alpha_3}{2} - \frac{1}{32}\right)\bar{\beta}^{-3/2} + \mathcal{O}\left(\bar{\beta}^{-5/2}\right). \tag{11}$$

4.2. Inner Solution

On the interval $0 \leqslant y < y_*$, we know that the solution slope is initially $-\gamma$ and so it is natural to introduce a new independent variable

$$r = \gamma y,$$

and define the inner solution as $u(r) = \Theta(y)$. Rescaling Eqs. (6′) yields

$$u\,u'' = -\frac{r\,u'}{\gamma^2}, \tag{12a}$$

$$u(0) = 1, \tag{12b}$$

$$u'(0) = -1. \tag{12c}$$

The $1/\gamma^2$ factor on the right hand side of (12a) suggests that if γ is large then we should use an asymptotic expansion of the form

$$u(r) = u_0(r) + \frac{u_1(r)}{\gamma^2} + \frac{u_2(r)}{\gamma^4} + \mathcal{O}\left(\frac{1}{\gamma^6}\right). \tag{13a}$$

After substituting this expression into the ODE and boundary conditions for u, we obtain the following sequence of initial value problems up to $\mathcal{O}\left(\gamma^{-4}\right)$:

$$\begin{aligned}
&u_0\,u_0'' = 0, && u_0(0) = 1, \quad u_0'(0) = -1,\\
&u_0\,u_1'' = -r u_0', && u_1(0) = 0, \quad u_1'(0) = 0,\\
&u_0\,u_2'' = -u_1 u_1'' - r u_1', && u_2(0) = 0, \quad u_2'(0) = 0.
\end{aligned}$$

These problems can be integrated successively to obtain

$$u_0 = 1 - r, \tag{13b}$$

$$u_1 = \frac{1}{2} - \frac{1}{2}(1-r)^2 + (1-r)\,\log(1-r), \tag{13c}$$

$$u_2 = \frac{17}{12} - \frac{3}{4}(1-r) - \frac{3}{4}(1-r)^2 + \frac{1}{12}(1-r)^3 + \left(2 - \frac{3}{2}r\right)\,\log(1-r), \tag{13d}$$

which after substitution into (13a) gives the inner solution to $\mathcal{O}\left(\gamma^{-4}\right)$. The $\mathcal{O}\left(1\right)$ and $\mathcal{O}\left(\gamma^{-2}\right)$ solutions are depicted in Figure 6 for values of $\bar{\beta} = 2$, 4 and 8. Plots of the numerical solution of Eqs. (6′), computed using the shooting algorithm described in Section 6 (and labeled "Exact") have also been included for comparison purposes.

We now investigate more carefully the validity of these asymptotic expressions. It is immediately clear that for asymptotic regularity we should have

$$u_0(r) \gg \frac{u_1(r)}{\gamma^2}.$$

Taking the leading order term on each side of this equation yields

$$(1-r) \gg \frac{1}{2\gamma^2}. \tag{14}$$

Finally, we discuss how the first two terms in the asymptotic expansion (13) may be used to give a first estimate the wetting front location y_*. To this end, we set $u_0 + u_1/\gamma^2 = 0$ and neglect terms that are quadratic and logarithmic in $(1-r)$ to obtain

$$r_* \approx 1 + \frac{1}{2\gamma^2} \qquad \text{or} \qquad y_* \approx \frac{1}{\gamma} + \frac{1}{2\gamma^3}, \tag{15}$$

which yields the first two terms in the front location (7). We also note that setting $r = 1$ yields the leading order estimates

$$u(1) \approx \frac{1}{2\gamma^2} \qquad \text{and} \qquad u'(1) = -1, \tag{16}$$

which will be useful in later scaling arguments. One of the primary aims of the more careful asymptotic matching performed in Section 4.3.3 is to derive a correction to Eq. (15) that gives more refined estimates of $u(1)$ and r_* to verify the above rough calculation.

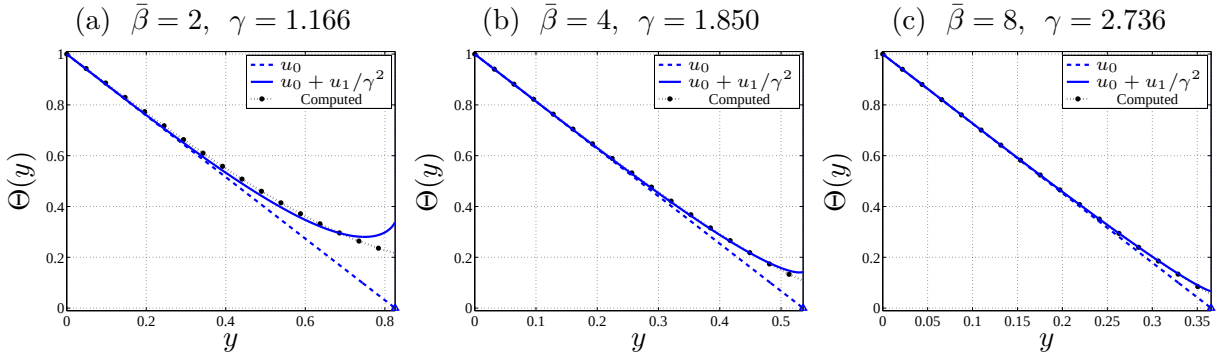

Figure 6. The inner solution $u(r)$ for values of $\bar{\beta} = 2$, 4 and 8, showing the leading order approximation u_0, first order correction $u_0 + u_1/\gamma^2$, and numerical solution of the ODE initial value problem. The point where the approximation u_0 touches the y–axis ($\triangle$) corresponds to the leading order estimate of the wetting front location, $y_* \approx 1/\gamma$.

4.3. Intermediate Layer

4.3.1. Preliminary Estimate of Leading Order Asymptotics and Solution Scalings. As $r \to 1$ we start to see the rapid transition between the linear solution and the exponentially small solution. We note that a standard application of the maximum principle in the intermediate region shows that $u(r) > 0$ and $u' < 0$ for all r, so that $u \to u_\infty \equiv \Theta_\infty$ and $u' \to 0$ as $r \to \infty$. This transition occurs over a narrow layer, which we will see is of width $\mathcal{O}\left(1/\gamma^2\right)$. Before getting into the detailed analysis of intermediate solution, we begin with some simple calculations that aim to establish the

leading order asymptotic form of the solution in intermediate layer close to the wetting front at r_* and also to estimate the width of this layer. These calculations will guide our more sophisticated calculations given later. Using the scalings in the inner region, we have

$$uu'' = -\frac{ru'}{\gamma^2}, \quad u(0) = 1, \quad u'(1^-) = -1, \quad u(\infty) = u_\infty \equiv \Theta_\infty. \tag{17}$$

If we now divide both sides of the ODE by ru, then integrate and apply the boundary conditions, we obtain

$$-\log(u_\infty) = \gamma^2 \int_0^\infty \frac{u''(r)}{r}\, dr. \tag{18}$$

In the case when γ is large, our previous estimates of the inner solution, combined with the numerical calculations, imply that:

(a) $u' \approx -1$ if $0 \leqslant r < r_*$; (b) $u' \approx 0$ if $r > r_*$; (c) $u'' \approx 0$ if $r \neq r_*$; and (d) $u''(r_*) \gg 1$.

It follows from these observations that

$$\gamma^2 \int_0^\infty \frac{u''}{r}\, dr \approx \gamma^2 \int_{r_*^-}^{r_*^+} \frac{u''}{r}\, dr \approx \gamma^2 \Big[\frac{u'}{r}\Big]_{r_*^-}^{r_*^+} \approx \frac{\gamma^2}{r_*},$$

which can be combined with (18) and the inner solution estimate $r_* = 1 + \mathcal{O}(1/\gamma^2)$ to obtain to leading order

$$-\log u_\infty \approx \gamma^2. \tag{19}$$

While this estimate for u_∞ is not precise, we can use this simple calculation as a guide in the subsequent development of the asymptotic theory.

For our next estimate, we make the assumption that as u'' is exponentially large only close to r_*, the leading order behaviour of the integral in (18)) can be approximated by freezing the value of $r = r*$ in the denominator of this integral. By integrating and applying the previous result, we obtain the leading order equation

$$-\frac{\gamma^2 u'}{r_*} = \log\left(\frac{u}{u_\infty}\right). \tag{20}$$

This equation can be integrated exactly when $r > 1$ to obtain

$$r_*\,(r-1) = \gamma^2 u_\infty \left[\mathrm{li}\left(\frac{u(1)}{u_\infty}\right) - \mathrm{li}\left(\frac{u}{u_\infty}\right)\right], \tag{21}$$

where

$$\mathrm{li}(z) = \int_0^z \frac{dt}{\log t}$$

is the *logarithmic integral function*. In order to determine the leading order behaviour in the intermediate layer $r \approx 1$ and to match with the inner and outer solutions, we consider the limit $u(r)/u_\infty \to 1$. From (16), we have that $u(1) \approx 1/2\gamma^2$ and $u_\infty \approx \exp(-\gamma^2)$, so that $u(1)/u_\infty \gg 1$ for large γ. To calculate the solution thus requires estimates of the logarithmic integral $\mathrm{li}(z)$ in the two limits $z \to 1$ and $z \to \infty$, which are well-known to be

$$\mathrm{li}(z) = \Gamma_e + \log\log z + \mathcal{O}\left(\log z\right) \qquad \text{as} \quad z \to 1, \tag{22}$$

$$\mathrm{li}(z) = \frac{z}{\log z} + \frac{z}{\log^2 z} + \mathcal{O}\left(\frac{z}{\log^3 z}\right) \quad \text{as} \quad z \to \infty, \tag{23}$$

where $\Gamma_e = 0.5772156649\ldots$ is the Euler-Mascheroni constant. Using the expansion (23) for large z, we obtain

$$\begin{aligned}\gamma^2 u_\infty \,\mathrm{li}\left(\frac{u(1)}{u_\infty}\right) &= \gamma^2 \frac{u(1)}{\log(u(1)) - \log(u_\infty)} + \mathcal{O}\left(\frac{\gamma^2 u(1)}{\log^2(u_\infty)}\right) \\ &= \frac{1}{2\gamma^2} + \mathcal{O}\left(\frac{1}{\gamma^4}\right)\end{aligned} \tag{24}$$

If we now let u/u_∞ be close to one, so that we are very close to the wetting front, and then combine the various expressions above, we have

$$r_*(r-1) = \frac{1}{2\gamma^2} + \mathcal{O}\left(\frac{1}{\gamma^4}\right) - \gamma^2 u_\infty \Big(\Gamma_e + \log\log(u/u_\infty)\Big). \tag{25}$$

Because $r_* = 1 + \mathcal{O}\left(1/\gamma^2\right)$, this is equivalent to

$$u = u_\infty \exp\exp\left(-\gamma^{-2} u_\infty^{-1}\left(r - 1 - \frac{1}{2\gamma^2} - \mathcal{O}\left(\frac{1}{\gamma^4}\right)\right) - \Gamma_e\right). \tag{26}$$

If (as consistent with our earlier estimates) we identify the term $1 + \frac{1}{2\gamma^2} + \mathcal{O}\left(\frac{1}{\gamma^4}\right)$ in this expression with the wetting front at r_*, we then have

$$u = u_\infty \exp\exp\Big(-\frac{r - r_*}{\gamma^2 u_\infty} - \Gamma_e\Big). \tag{27}$$

The structure of the intermediate layer is now clear. Because $u_\infty^{-1} \approx e^{\gamma^2}$ is very large indeed, there is a very rapid transition from the inner solution where $u' \approx -1$ to the solution $u = u_\infty, u' = 0$ as we pass through the wetting front, over a range $\Delta r \approx \gamma^2 e^{-\gamma^2}$.

4.3.2. Left Intermediate Solution. Guided by the above, we now refine the asymptotic calculation in the intermediate layer, in particular for the range $r < 1 + 1/2\gamma^2 + \mathcal{O}(1/\gamma^4)$, to get a more precise estimate of the location of the wetting front and of the value of u_∞. This calculation is rather technical, but allows us to obtain higher order asymptotic estimates which can then be compared with the numerical calculations. Within this range, we first determine an appropriate rescaling of the spatial variable r and dependent variable u by studying the form of the inner solution as $r \to 1^-$. In this limit, the dominant terms in the inner expansion (13) are

$$u(r) = 1 - r + \frac{1}{\gamma^2}\left(\frac{1}{2} + \ldots\right), \tag{28}$$

Consequently, we make introduce a new independent variable s that is $\mathcal{O}(1)$ and is given by

$$r = 1 + \frac{s}{\gamma^2} \tag{29}$$

We note that taking s large and negative (for example $\mathcal{O}(\gamma)$) allows us to match to the inner solution. Furthermore, the results of the previous section show that there is very rapid convergence to the outer solution, with $u \to u_\infty$, for $s > 1/2 + \mathcal{O}(1/\gamma^2)$. We are motivated by considerations of matching to define a new intermediate-range saturation variable $v(s)$ via

$$u(r) = \frac{v(s)}{\gamma^2},$$

so that

$$u'(1^-) = v'(-\infty) \quad \text{and} \quad u(1^-) \approx \frac{1}{2\gamma^2} \quad \text{imply} \quad v(0) \approx \frac{1}{2}.$$

We then have to leading order

$$v\, v'' = -\frac{v'}{\gamma^2}\left(1 + \frac{s}{\gamma^2}\right). \tag{30}$$

As s increases the intermediate-range solution will match rapidly to the outer solution so that

$$v(s) \to v_\infty := \gamma^2 u_\infty, \quad v'(s) \to 0 \quad \text{if} \quad s > s_* = 1/2 + \mathcal{O}(1/\gamma^2). \tag{31}$$

Integrating Eq. (30) over the interval $[s, s_*^+)$ yields

$$\gamma^{-2}\Big(\log(v(s)) - \log(v_\infty)\Big) = \int_s^{s_*} \frac{v''\, ds}{(1 + s/\gamma^2)}.$$

We will assume that the the range of s is restricted to

$$s/\gamma^2 \ll 1,$$

so that the denominator in the integrand may be expanded as a geometric series and

$$\gamma^{-2}\Big(\log(v(s)) - \log(v_\infty)\Big) = \int_s^{s_*} v''\left(1 - \frac{s}{\gamma^2} + \mathcal{O}\left(\frac{s^2}{\gamma^4}\right)\right) ds.$$

Using integration by parts and applying the far field condition $v' \to 0$ for s_*^+, we find that

$$\gamma^{-2}\Big(\log(v) - \log(v_\infty)\Big) = -v'\left(1 - \frac{s}{\gamma^2}\right) + \frac{(v_\infty - v)}{\gamma^2} + \mathcal{O}\left(\frac{1}{\gamma^4}\right),$$

which can be rearranged to obtain

$$v' = \gamma^{-2}\Big(\log(v_\infty) - \log(v)\Big) + \frac{s v'}{\gamma^2} + \frac{1}{\gamma^2}(v_\infty - v) + \mathcal{O}\left(\frac{1}{\gamma^4}\right). \tag{32}$$

We now carefully consider the solution of this equation for $s < 1/2$ and match it to the inner solution. This calculation is rather technical and involved, however it furnishes very precise information about the value of Θ_∞ and the wetting front location. To do this we develop an asymptotic expression of the form

$$v(s) = v_0(s) + \frac{v_1(s)}{\gamma^2} + \frac{v_2(s)}{\gamma^4} + \ldots \quad \text{when} \quad s < \frac{1}{2} + \mathcal{O}(1/\gamma^2). \tag{33}$$

A subtle feature of this expansion follows from the coexistence of the logarithmic and polynomial expressions in both the intermediate layer expansion and the inner solution. This means that in order to capture the solution behaviour it is necessary that $v_1(s)$ has terms of both $\mathcal{O}(1)$ and $\mathcal{O}(\log\gamma)$. However, provided that γ is large, this means that we still have $v_0 \gg v_1/\gamma^2 \gg v_2/\gamma^4$ so that the formal nature of the asymptotic series is preserved. We assume further, motivated by the previous analysis, that

$$v(0) = \frac{1}{2} + a\frac{\log\gamma}{\gamma^2} + \frac{b}{\gamma^2} + \mathcal{O}\left(\frac{1}{\gamma^4}\right), \tag{34}$$

$$\log v_\infty = -\gamma^2 + c\log\gamma + d + \mathcal{O}\left(\frac{1}{\gamma^2}\right), \tag{35}$$

and we will determine explicit values for the constants a, b, c, d. We next substitute the expressions (33)–(35) into (32) and solve the equations arising at each order.

Considering first the leading terms of $\mathcal{O}(1)$, we find that

$$v_0{}' = -1, \qquad v_0(0) = \frac{1}{2},$$

which has solution

$$v_0(s) = \frac{1}{2} - s. \tag{36}$$

Next, take the terms of $\mathcal{O}\left(1/\gamma^2, \log\gamma/\gamma^2\right)$ for which we first need to expand $\log v$ from Eq. (32) as a series in γ

$$\log v = \log\left(\left(\frac{1}{2} - s\right) + v_1/\gamma^2 + \cdots\right) = \log\left(\frac{1}{2} - s\right) + \mathcal{O}\left(\frac{1}{\gamma^2}\right),$$

where we have used the fact that $v_0 > 0$ when $s < 1/2$. The $\mathcal{O}\left(1/\gamma^2, \log\gamma/\gamma^2\right)$ terms in the intermediate layer expression then become

$$v_1{}' = c\ \log\gamma + \left(d - \frac{1}{2}\right) - \log\left(\frac{1}{2} - s\right),$$

which can be integrated to obtain

$$v_1(s) = c\, s\log\gamma + \left(d - \frac{1}{2}\right)s + a\log\gamma + b + \left(\frac{1}{2} - s\right)\log\left(\frac{1}{2} - s\right) + s - \frac{1}{2}\log 2. \tag{37}$$

We now match the intermediate range expansion $v = v_0 + v_1/\gamma^2 + \mathcal{O}\left(1/\gamma^4\right)$ to the inner solution when $s < 0$ and $|s| = \mathcal{O}(\gamma) \gg 1$. Making use of the expansion

$$\left(\frac{1}{2} - s\right)\log\left(\frac{1}{2} - s\right) = \left(\frac{1}{2} - s\right)\log(-s) + \frac{1}{2} + \mathcal{O}\left(\frac{1}{s}\right),$$

we can write the intermediate-range solution with terms ordered by size (for this range of s) as

$$v(s) = \left(\frac{1}{2} - s\right) + \frac{1}{\gamma^2}\left(\frac{1}{2} - s\right)\log(-s) + c\, s\frac{\log\gamma}{\gamma^2} + \frac{1}{\gamma^2}\left(d + \frac{1}{2}\right)s + a\frac{\log\gamma}{\gamma^2} + \frac{b}{\gamma^2} + \frac{1}{\gamma^2}\frac{1}{2}(1 + \log 2) + \mathcal{O}\left(\frac{1}{\gamma^2 s}, \frac{1}{\gamma^4}\right). \tag{38}$$

Next, rewrite the inner solution (13) using $v = \gamma^2 u(r)$ and

$$r = 1 + \frac{s}{\gamma^2}.$$

Then, for $|s| = \mathcal{O}(\gamma)$, we obtain the inner expansion in terms of the intermediate range variable as

$$\gamma^2 u\left(1 + \frac{s}{\gamma^2}\right) = \left(\frac{1}{2} - s\right) - \frac{1}{\gamma^2}s\log(-s) + 2s\frac{\log\gamma}{\gamma^2} + \frac{17}{12\gamma^2} + \frac{1}{\gamma^2}\frac{1}{2}\log(-s) - \frac{\log\gamma}{\gamma^2} + \mathcal{O}\left(\frac{1}{\gamma^4}\right).$$

By comparing this expression with that for the intermediate range in (38), we find that all terms match (both constant and logarithmic) provided the constants satisfy the identities

$$a = -1, \qquad b = \frac{11}{12} - \frac{1}{2}\log 2, \qquad c = 2, \qquad d = -\frac{1}{2}.$$

Therefore, the intermediate-range solution for $s < 1/2$ is given asymptotically by

$$v(s) = \left(\frac{1}{2} - s\right) + (2s-1)\frac{\log\gamma}{\gamma^2} + \frac{11}{12\gamma^2} + \frac{1}{\gamma^2}\left(\frac{1}{2} - s\right)\log\left(\frac{1}{2} - s\right) + \mathcal{O}\left(\frac{1}{\gamma^4}\right), \tag{39}$$

which we can write as

$$v(s) = \left(\frac{1}{2} + \frac{11}{12\gamma^2} - s\right)\left(1 + \frac{-2\log(\gamma) + \log(1/2 - s)}{\gamma^2}\right) + \mathcal{O}\left(\frac{1}{\gamma^4}\right). \tag{40}$$

Substituting the constants into (34), we also find that to leading order

$$v(0) = \frac{1}{2} + \frac{b - \log(\gamma)}{\gamma^2} + \mathcal{O}\left(\frac{1}{\gamma^4}\right) \qquad \text{or} \qquad u(1) = \frac{1}{2\gamma^2} + \frac{b - \log\gamma}{\gamma^4} + \mathcal{O}\left(\frac{1}{\gamma^6}\right). \tag{41}$$

Similarly, (35) implies that

$$\log v_\infty = -\gamma^2 + 2\log\gamma - \frac{1}{2} + \mathcal{O}\left(\frac{1}{\gamma^2}\right),$$

so that

$$v_\infty = \gamma^2 e^{-\gamma^2 - 1/2 + \mathcal{O}(1/\gamma^2)} \qquad \text{or} \qquad \Theta_\infty = u_\infty = e^{-\gamma^2 - 1/2 + \mathcal{O}(1/\gamma^2)}. \tag{42}$$

4.3.3. A More Precise Estimate of Front Location and Solution Curvature. The expression (40), in which $v(s)$ would appear to vanish when $s = 1/2 + 11/12\gamma^2 + \mathcal{O}\left(1/\gamma^4\right)$, is strongly suggestive of a wetting front location given in terms of the inner variable by

$$r_* = 1 + \frac{1}{2\gamma^2} + \frac{11}{12\gamma^4} + \mathcal{O}\left(\frac{1}{\gamma^6}\right). \tag{43}$$

To further support this estimate, we return to the expression (21) for the overall behaviour of the solution in the intermediate layer, and continue the calculation given earlier using the more refined values for $u(1)$ and u_∞ given by (41) and (42). Expanding the $\mathrm{li}(z)$ function to include the $z/\log^2 z$ term, we obtain after some manipulation

$$\begin{aligned}\gamma^2 u_\infty \ \mathrm{li}\left(\frac{u(1)}{u_\infty}\right) &= \frac{\frac{1}{2} + \frac{1}{\gamma^2}\left(\frac{11}{12} - \frac{\log(2)}{2} - \log(\gamma)\right)}{\log(1/2\gamma^2) + \gamma^2 + 1/2} + \frac{1/2}{\gamma^4} + \mathcal{O}\left(\frac{1}{\gamma^6}\right), \\ &= \frac{1}{2\gamma^2} + \frac{11}{12\gamma^4} + \frac{1}{4\gamma^4} + \mathcal{O}\left(\frac{1}{\gamma^6}\right).\end{aligned}$$

Thus, as

$$r_*(r-1) = \gamma^2 u_\infty \ \mathrm{li}\left(\frac{u(1)}{u_\infty}\right) - \gamma^2 u_\infty \ \mathrm{li}\left(\frac{u(r)}{u_\infty}\right),$$

we have

$$\begin{aligned}(r-1) &= \frac{\frac{1}{2\gamma^2} + \frac{11}{12\gamma^4} + \frac{1}{4\gamma^4} + \mathcal{O}\left(\frac{1}{\gamma^6}\right)}{1 + \frac{1}{2\gamma^2} + \mathcal{O}\left(\frac{1}{\gamma^4}\right)} - \gamma^2 u_\infty \ \mathrm{li}\left(\frac{u(r)}{u_\infty}\right) \\ &= \frac{1}{2\gamma^2} + \frac{11}{12\gamma^4} + \mathcal{O}\left(\frac{1}{\gamma^6}\right) - \gamma^2 u_\infty \ \mathrm{li}\left(\frac{u(r)}{u_\infty}\right).\end{aligned}$$

We deduce that if r_* is now as given in (43), then with this refined value

$$r - r_* = -\gamma^2 u_\infty \ \mathrm{li}\left(\frac{u(r)}{u_\infty}\right). \tag{44}$$

Applying the previous reasoning, this leads to exactly the expression (27), with r_* now given by the refined approximation (43).

An alternative definition of the wetting front location is that it is the point r_{**} where the curvature u'' takes its maximum value, so that $u'''(r_{**}) = 0$. We now show that this is equivalent to the value r_* given above, and estimate the curvature at this point. Differentiating the underlying differential equation yields

$$uu''' + u'u'' = -ru''/\gamma^2 - u'/\gamma^2,$$

so that imposing $u'''(r_{**}) = 0$ yields at $r = r_{**}$

$$u' = -\frac{ru''}{1 + \gamma^2 u''}.$$

Assuming that $r_{**} \approx 1$ and $u''(r_{**}) \gg 1$, we have to leading order

$$u'(r_{**}) = -\frac{1}{\gamma^2}.$$

However, based on the intermediate range equation derived earlier, we also have

$$\gamma^2 u' = -\log\left(\frac{u}{u_\infty}\right),$$

and so it follows immediately that the maximum value of u'' arises when

$$\log\left(\frac{u}{u_\infty}\right) = 1 \qquad \text{or} \qquad u(r_{**}) = eu_\infty. \tag{45}$$

Substituting these various approximations into the underlying ODE we find that to leading order the maximum value of u'' at $r = r_{**}$ is given by

$$\max u'' \approx \frac{1}{\gamma^4 e u_\infty} = \frac{e^{\gamma^2 - 1/2}}{\gamma^2}. \tag{46}$$

As expected, this is very large indeed for even moderately large γ. This incidentally leads to severe problems in any numerical scheme that attempts to compute for large γ.

The wetting front location may now be estimated by substituting (45) into (44) to give

$$r_{**} - r_* = -\gamma^2 u_\infty \,\mathrm{li}(e).$$

Because $\mathrm{li}(e)$ is of order one, we have that r_{**} and r_* are identical to all polynomial orders.

4.4. Outer Solution, and Matching to the Intermediate Solution

To complete this calculation, we now match to the outer solution. We recall from (27) that the outer form of the intermediate range solution is given by

$$u = u_\infty \exp\exp\left(-\frac{(r - r_*)}{\gamma^2 u_\infty} - \Gamma_e\right). \tag{47}$$

We observe from this expression that u is very close to u_∞ if r is only *slightly larger* than r_*. In this range, the term $\exp\left(-\gamma^{-2}e^{\gamma^2}\left(r-r_*\right)-\Gamma_e\right)$ is very small, so that we may approximate (47) by

$$u = u_\infty\left[1+\exp\left(-\frac{(r-r_*)}{\gamma^2 u_\infty}-\Gamma_e\right)\right]. \tag{48}$$

Within the outer region, we have that $u \to u_\infty$ as $r \to \infty$. To match to the solution outer region, we take this to correspond to those r values for which u is close to u_∞ and look for a solution that is a small perturbation from a constant, namely

$$u(r) = u_\infty(1+g(r)), \tag{49}$$

where both $|g|$, $|g'| \ll 1$ for y sufficiently large. After substituting this expression into (6a), we obtain

$$\gamma^{-2}g' = -\frac{u_\infty}{r}\left(1+g\right)g'',$$

which can be approximated for small $|g|$ by

$$u_\infty g'' = -\gamma^{-2}rg'.$$

This equation can be integrated once to obtain

$$g' = -A\exp\left(-\frac{\left(r^2-r_*^2\right)}{2u_\infty\gamma^2}\right), \tag{50}$$

where $A>0$ is a constant. Close to r_* we then have

$$g' = -A\exp\left(-\frac{r_*(r-r_*)}{u_\infty\gamma^2}\right). \tag{51}$$

Because $r_*=1$ to leading order, this expression for g' exactly matches the derivative of the expression (48) as long as

$$A = \frac{e^{-\Gamma_e}}{u_\infty\gamma^2}. \tag{52}$$

This completes the outer solution matching to leading order.

4.5. Asymptotic Expansion for γ

We have so far expressed all asymptotic expansions in terms of the large parameter γ. However, γ is not actually known *a priori* for a physical problem and so instead it is preferable to write γ in terms of the known parameter $\bar{\beta}$. Taking the result from (42), we have that

$$\bar{\beta} = \gamma^2+\frac{1}{2}+\frac{\alpha_3}{\gamma^2}+\mathcal{O}\left(\frac{1}{\gamma^4}\right), \tag{53}$$

where we have introduced the coefficient α_3 that is yet to be determined. Neglecting the $\mathcal{O}\left(\gamma^{-4}\right)$ terms yields a quadratic equation for γ^2 whose solution can be expressed for large $\bar{\beta}$ as

$$\gamma = \bar{\beta}^{1/2}-\frac{1}{4}\bar{\beta}^{-1/2}-\left(\frac{\alpha_3}{2}+\frac{1}{32}\right)\bar{\beta}^{-3/2}+\mathcal{O}\left(\bar{\beta}^{-5/2}\right). \tag{54}$$

The high fidelity numerical calculations reported by Amodio et al. [24] provide convincing numerical evidence that

$$\alpha_3 = \frac{1}{12},$$

although we have no formal calculation as yet to confirm this result.

4.6. Summary of Composite Asymptotic Solution

Here we present a concise summary of the leading order asymptotic approximations for the inner, intermediate and outer solutions derived in Eqs. (13), (39), (48), (49), (50) and (52), expressing each in terms of the original similarity variables y and $\Theta(y)$ as follows:

$$\text{Inner:}\quad (0 \leqslant y < \gamma^{-1}) \qquad \Theta(y) = 1 - \gamma y + \frac{1}{\gamma^2}\left[\frac{1}{2} - \frac{1}{2}(1-\gamma y)^2 + (1-\gamma y)\log(1-\gamma y)\right] + \mathcal{O}\left(\frac{1}{\gamma^4}\right), \tag{55a}$$

$$\text{Left intermediate:}\quad (\gamma^{-1} < y < y_*) \qquad \Theta(y) = \frac{1}{\gamma}(y_* - y)\left[\gamma^2 + \log\gamma + \log(y_* - y)\right] + \mathcal{O}\left(\frac{1}{\gamma^3}\right), \tag{55b}$$

$$\text{Right intermediate:}\quad (y > y_*) \qquad \Theta(y) \approx \Theta_\infty + \Theta_\infty \exp\left(-\Gamma_e - \frac{y - y_*}{\gamma\Theta_\infty}\right), \tag{55c}$$

$$\text{Outer:}\quad (y \to \infty) \qquad \Theta'(y) \approx \frac{1}{\gamma}\frac{e^{-\Gamma_e}}{\Theta_\infty}\exp\left(-\frac{y^2 - y_*^2}{2\Theta_\infty}\right). \tag{55d}$$

In these above expressions, $\Theta_\infty = e^{-\bar{\beta}}$ and γ can be written in terms of $\bar{\beta}$ as

$$\gamma \approx \bar{\beta}^{1/2} - \frac{1}{4}\bar{\beta}^{-1/2} - \left(\frac{\alpha_3}{2} + \frac{1}{32}\right)\bar{\beta}^{-3/2}. \tag{55e}$$

This last equation may also be used to replace γ in the expansion of the front location (43) to yield

$$y_* \approx \bar{\beta}^{-1/2} + \frac{3}{4}\bar{\beta}^{-3/2} + \left(\frac{\alpha_3}{2} + \frac{133}{96}\right)\bar{\beta}^{-5/2}, \tag{55f}$$

where $\alpha_3 = \frac{1}{12}$ (numerically).

5. Other Asymptotic Approximations

In this section, we present two alternate asymptotic solutions to the exponential diffusion problem that are derived using other methods.

5.1. Babu's Solution

Babu [16] studied a modified version of the exponential diffusion problem in which he assumed that beyond some distance $y \geqslant y_*$ the saturation is equal to the residual value. In other words, he solves a modified boundary value problem that replaces our condition at infinity (6c) with

$$\Theta(y_*) = \Theta_\infty \qquad \text{and} \qquad \frac{d\Theta}{dy} \to 0 \quad \text{as } y \to y_*. \tag{6c$''$}$$

Here, the front location y_* is an unknown constant that must be determined as part of the solution, which explains the need for the extra limiting condition in (6c″) that corresponds physically to requiring a zero water flux at y_*. By expanding the solution as a series in $\eta = (1 - \Theta_\infty)/\bar{\beta}$, Babu obtained the following approximation for the wetting front location

$$y_*^B = \eta^{1/2} \left[1 + \frac{1}{3}\eta + \left(\frac{17}{90} + \frac{\bar{\beta}}{8} \right) \eta^2 + \cdots \right], \tag{56a}$$

where we use a superscript "B" to distinguish Babu's solution. Neglect exponentially small terms in $\Theta_\infty = e^{-\bar{\beta}}$, this expression may be rewritten in terms of $\bar{\beta}$ as

$$y_*^B \approx \bar{\beta}^{-1/2} + \frac{11}{24}\bar{\beta}^{-3/2} + \mathcal{O}\left(\bar{\beta}^{-5/2}\right), \tag{56b}$$

which may then be compared directly to our asymptotic approximation in (55f). Although the leading order terms in $\mathcal{O}\left(\bar{\beta}^{-1/2}\right)$ are identical, the difference in coefficients at the next order generates a significant discrepancy in the front locations. Babu also derived two further approximations that he refers to as second- and third-order expansions

$$\Theta^{B,2}(y) = 1 + \bar{\beta}\eta^{1/2} \left(\frac{\eta}{6}\, y - y + \frac{1}{6}\, y^3 \right), \tag{56c}$$

$$\Theta^{B,3}(y) = \Theta^{B,2}(y) + \bar{\beta}\eta^{1/2} \left[\left(\frac{7}{360} + \frac{\bar{\beta}}{24} \right) \eta^2 y - \frac{\eta}{36} y^3 + \frac{\bar{\beta}\eta^{1/2}}{12} y^4 - \frac{1}{40} y^5 \right], \tag{56d}$$

both of which are defined on the interval $0 \leqslant y \leqslant y_*^B$. When $y > y_*^B$, the saturation in both cases satisfies $\Theta^{B,2} = \Theta^{B,3} = \Theta_\infty$ (corresponding to $\bar{\theta} = 0$). Babu's solution is simpler than the one derived in this paper in that it is a polynomial expansion in integer powers of y and requires no multi-layer matching. However, this simplicity comes at the expense of reduced accuracy as well as a lack of information about the detailed structure of the wetting front. Another disadvantage of Babu's approach is that none of his approximations for Θ is continuous at $y = y_*^B$.

5.2. Parlange's Solution

Many approaches for solving the nonlinear diffusion equation analytically begin with the *Bruce-Klute equation*, $D(\theta) = -\frac{dy}{d\theta} \int_{\theta_\circ}^{\theta} y(\alpha)\, d\alpha$, which can be derived from (6) by treating y as a function of saturation θ [25]. Although this equation was originally used to help interpret experimental data, it has subsequently been exploited by many authors to derive analytical solutions of the nonlinear diffusion equation, most notably by Philip [26, 27]. A related iterative solution approach was developed by Parlange [28, 17], who applied a number of simplifications to obtain an approximate formula for y in terms of integrals of the diffusivity. For the specific case of an exponential diffusivity, Parlange [17] derived an implicit asymptotic representation for the saturation that can be expressed in our similarity variables as

$$y = \left(\bar{\beta}^{-1/2} + \bar{\beta}^{-3/2} \right) \left(1 - \Theta^P + \Theta^P \log \Theta^P / \bar{\beta} \right). \tag{57a}$$

In a similar manner to Babu, Parlange also imposed the condition that $\Theta \equiv \Theta_\infty = e^{-\bar{\beta}}$ for all $y \geqslant y_*^P$. Equating terms in Eq. (57a) gives the result

$$y_*^P = \left(\bar{\beta}^{-1/2} + \bar{\beta}^{-3/2} \right) \left(1 - 2e^{-\bar{\beta}} \right). \tag{57b}$$

Intriguingly, this estimate involves an exponential term that would correspond to a "beyond all orders" contribution to the results in this paper. This estimate behaves asymptotically in the limit of large $\bar{\beta}$ as

$$y_*^P \approx \bar{\beta}^{-1/2} + \bar{\beta}^{-3/2}, \tag{58}$$

from which it is clear that the front location matches only at leading order with our estimate (55f) and that of Babu from (56b).

Another related solution was derived from the Bruce-Klute equation by Parlange et al. [18], who extended an earlier method of Heaslet and Alksne [29] for the power-law diffusivity to the exponential case. This solution also has representation for Θ that involves the exponential integral function, $\mathrm{Ei}(z)$. Because evaluating Θ requires inverting Ei, their solution is much more complicated and expensive to compute than ours and so we have not considered it here.

6. Comparison of Asymptotic and Numerical Results

We now compare the various asymptotic solutions presented in the preceding sections. We also validate the asymptotic results using numerical simulations of the initial value problem in Eqs. (6′) based on an algorithm that is described next.

6.1. Solution Algorithm

The ODE (6a) for the similarity variable $\Theta(y)$ is solved numerically over an interval $y \in [0, M]$ using the MATLAB initial value solver `ode15s`. Because both the problem and our asymptotic results correspond to the semi-infinite interval $[0, \infty]$, we must choose M sufficiently large that any error arising from truncating the right-hand boundary does not pollute the solution in the interior; on the other hand, $\Theta(y)$ tends quite rapidly toward Θ_∞ as y increases beyond the front, and so M does not need not be taken much larger than y_*. In practice, we have found that choosing $M = 2\bar{\beta}^{-1/2}$ (twice the leading order estimate of the wetting front location) provides a reasonable compromise between efficiency and accuracy.

For an actual wetting scenario, we know the asymptotic saturation Θ_∞ (from $\bar{\beta}$), but the value of γ in the second initial condition is not known *a priori*. We therefore build the initial value solver into a shooting type algorithm, for which we guess the value $\gamma = -\Theta'(0)$, integrate the saturation variable to $\Theta(M)$, and then compare to the target value Θ_∞. The value of γ is then modified using the bisection method and this integration procedure is iterated until the relative error in the right boundary condition satisfies $|\Theta(M) - \Theta_\infty|/\Theta_\infty < \texttt{TOL}$, where `TOL` is a given tolerance. The leading term $\gamma \approx \bar{\beta}^{1/2}$ from the asymptotic formula (55e) provides a sufficiently accurate initial guess to begin the iteration, and choosing ODE tolerances of $\texttt{ABSTOL} = \texttt{RELTOL} = 10^{-10}$ and Θ-tolerance of $\texttt{TOL} = 10^{-6}$ yields a computed solution that for all intents and purposes can be treated as an "exact solution" of the original problem.

A significant difficulty with this algorithmic approach is that for even moderate values of γ the solution curvature near the wetting front is on the order of $\exp(\gamma^2)$, which can be extremely large. This large curvature causes problems with the initial value solver we are using, and effectively limits the maximum value of $\bar{\beta}$ to roughly 20, which restricts $\gamma \lessapprox 4.4$. With this restricted range of γ, we can still test the validity of the asymptotic formulae derived here but we are not able to see their true accuracy at larger γ, as the asymptotic series we have derived only converge at a polynomial rate as γ increases. Consequently, we will also report some results using a much more sophisticated numerical approach that is the subject of a related paper [24] and which employs a high-order

Taylor expansion based boundary value solver coupled with mesh adaptivity. This method permits calculations up to $\gamma = 18$, corresponding to $\bar{\beta} \approx 325$ and $\theta_\infty \approx 1.18 \times 10^{-141}$.

6.2. Saturation Profiles

Plots of the multi-layer asymptotic solution determined by Eqs. (55) are depicted in Figure 7 for values of $\bar{\beta} = 4$, 8 and 16 alongside the corresponding plots of the computed solution using the shooting method described above (which can essentially be considered as an "exact solution"). The inner and intermediate-range solution are both displayed, and the loss of asymptotic validity of the inner solution due to the logarithmic term is evident as $y \to y_*$. We have included in all plots the corresponding asymptotic solutions of Babu [16] and Parlange [17], and in each case a second plot of all curves in terms of the rescaled saturation $\bar{\theta}$ is given (lower plots), which accentuates differences in the wetting front location. Our asymptotic solution is clearly an improvement over Babu's solution for all values of $\bar{\beta}$, which we attribute in large part to the fact that Babu's approximation truncates the saturation at some approximate wetting front location and ignores the details of the solution structure within and to the right of the front.

As described above, the relatively slow convergence of our asymptotic solution, which is polynomial in γ, and hence also in $\bar{\beta}$, means that our asymptotic approximation is not particularly accurate for smaller values of $\bar{\beta}$ such as $\bar{\beta} = 4$. This is reflected in the mismatch between the left and right intermediate-range solutions at the wetting front location (represented by the blue triangular point). However, our asymptotic approximation improves significantly in accuracy as $\bar{\beta}$ increases, and when we take $\bar{\beta} = 16$ the comparison between the computed and asymptotic results are good. The differences at even larger $\bar{\beta}$ are difficult to visualize using saturation plots, and so we compare the solutions further in the next sections in terms of the estimates for wetting front location.

6.3. Wetting Front Location, y_*

We next focus on calculations of the wetting front location y_*, which we have defined in our derivation to the be point where Θ'' is a maximum. A visual comparison is provided in Figure 8 in terms of the computed front location as a function of $\bar{\beta}$, showing our asymptotic estimate y_*^{asy} from (55f), Babu's estimate y_*^B given in (56d), and Parlange's estimate y_*^P given in (58). We also included numerical estimates of front location using the Matlab solver `ode15s`, for which we were able to compute up to a maximum of $\bar{\beta} \approx 20$ before the ODE solver failed. The plot of error in front location (relative to the computed solution) clearly shows that although Parlange's estimate is better than our asymptotic solution for some values of $\bar{\beta} \gtrapprox 10$, our result is consistently superior for larger $\bar{\beta}$; indeed, even our two-term asymptotic solution surpasses Parlange's result when $\bar{\beta} \gtrapprox 13$.

Although our simple numerical approach fails for $\bar{\beta} > 20$, a more sophisticated numerical algorithm has been implemented by Amodio et al. [24] that yields accurate solutions for values of $\bar{\beta}$ much larger. Their results for a much wider range of $\bar{\beta}$ are summarized in Table 1, along with the corresponding asymptotic results for y_*^{asy}, y_*^B and y_*^P. The superior accuracy of our asymptotic solution for large $\bar{\beta}$ when compared with Babu's and Parlange's approximations is evident upon comparing the computed value of y_* to the three asymptotic approximations.

6.4. Initial Slope, $-\gamma$

Finally, we investigate the accuracy of our asymptotic approximation for γ in Eq. (55e), where $-\gamma$ is the initial slope in the similarity variable Θ. No corresponding estimate is available from either Babu's or Parlange's solutions. For a range of $\bar{\beta}$, Figure 9 compares the value of γ determined

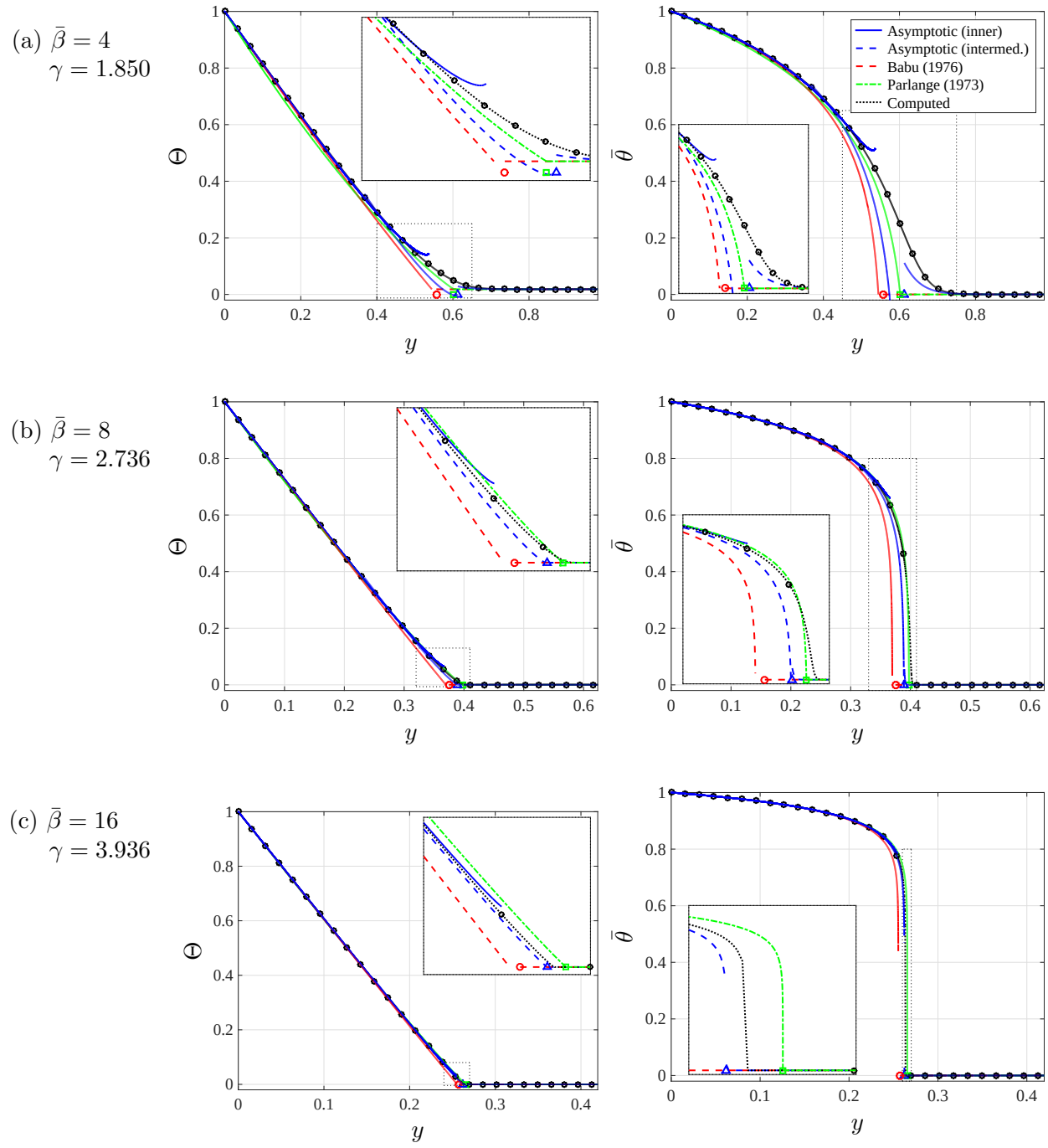

Figure 7. Comparison of our asymptotic solution (——) to those of Babu (– – –) and Parlange (-·-·-) for $\bar{\beta} = 4$, 8 and 16, displayed in terms of the similarity variable (left) and rescaled saturation (right). The corresponding approximations of the wetting front location are denoted by points lying on the y-axis for our asymptotics (△), Babu (○) and Parlange (□).

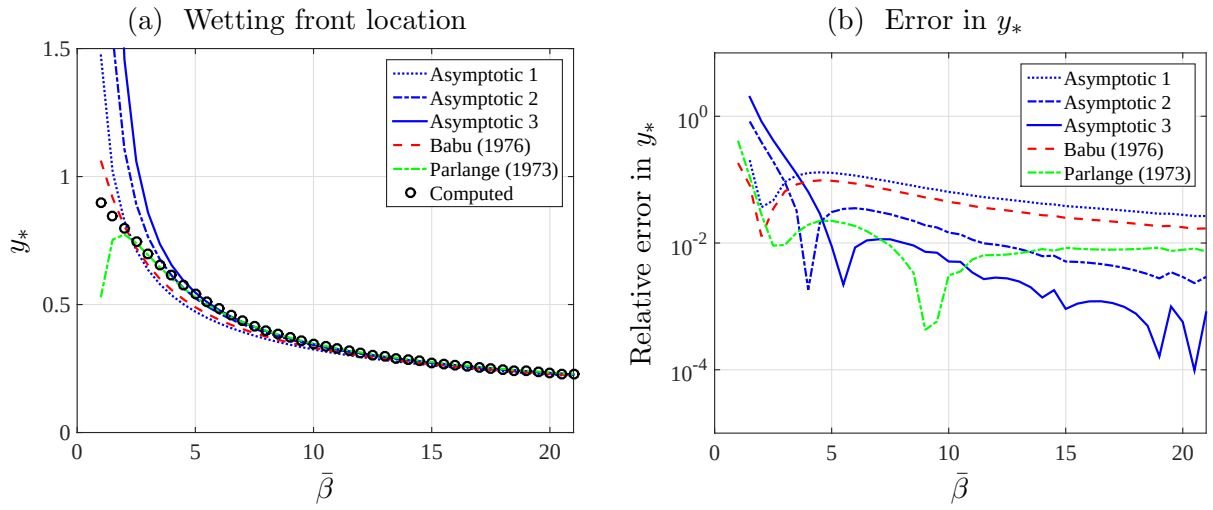

Figure 8. Comparison of the various asymptotic estimates for wetting front location y_* to the computed ("exact") solution.

Table 1

Comparison of our asymptotic results to computations using the method of Amodio et al. [24].

	Computed results			Asymptotic results		
γ	$\bar{\beta}$	θ_∞	y_*	y_*^{asy}	y_*^B	y_*^P
2	4.559435	1.046797e–2	0.571747	0.54536	0.51539	0.57103
6	36.50238	1.403505e–16	0.16911	0.1689165	0.16759	0.170050
10	100.5008	2.254440e–44	0.1005094	0.1004949	0.100205	0.100743
18	324.5002	1.178490e–141	0.0556417	0.0556410	0.0055591	0.055683

from shooting simulations with that obtained from the 1-, 2- and 3-term asymptotic estimates. The accuracy of our series approximation is evident for increasing values of $\bar{\beta}$, which is essential because γ is a required input for our numerical simulations and yet it is the parameter $\bar{\beta}$ (not γ) that is known *a priori* for any given physical wetting scenario.

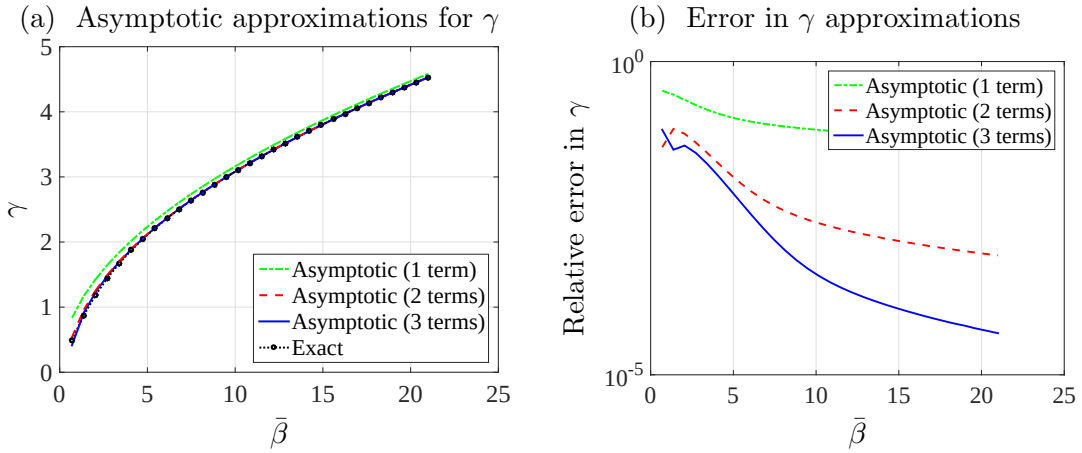

Figure 9. Comparison of the various asymptotic approximations of γ based on retaining one, two or three terms from the series in Eq. (55e). The left hand plot compares the three asymptotic results to the value of γ obtained using the shooting algorithm. The right hand plot depicts the corresponding absolute error in the asymptotic approximations, treating the shooting results as the "exact" solution.

We finish by restating some of the numerical results obtained in [24] for values of γ as high as 18 (corresponding to β up to 324). Beyond this range, even this more sensitive algorithm was unable to converge owing to the size of θ'' at the wetting front. The primary calculations of y_* and θ_∞ over a range of values of γ were then enhanced by using Richardson extrapolation. The primary contribution of [24] was to provide clear numerical evidence to support the validity of the following expressions

$$y_* \approx \frac{1}{\gamma} + \frac{1}{2\gamma^3} + \frac{11}{12\gamma^5} + \frac{2.96}{\gamma^7},$$

and

$$\bar{\beta} = -\log(\theta_\infty) \approx \gamma^2 + \frac{1}{2} + \frac{1}{12\gamma^2} + \frac{0.089}{\gamma^4},$$

which extends the asymptotics derived in this paper by one additional term. These results are in full agreement with our asymptotics and also hint at a more refined asymptotic calculation.

7. Conclusions

In this paper we have performed a multi-layer asymptotic analysis of a nonlinear diffusion equation where the diffusion coefficient is an exponential function, $D(\theta) = D_o e^{\beta\theta}$. We focus on an application to the study of wetting front formation in unsaturated porous media flow, although exponential diffusion also arises in a number of other problems in heat transport, optical lithography, polymer diffusion, etc. The original boundary value problem for liquid saturation is reformulated as an

initial value problem which, although not strictly necessary (c.f. Babu's solution [16] in Section 5.1), nonetheless permits an easy comparison to numerics using an initial value solver. Motivated by the structure of the wetting front for large values of β, we used the method of matched asymptotics to derive a four-layer solution consisting of a different asymptotic series for each of four regions corresponding to the wetting, and the leading and trailing edges. Other previous approaches to deriving (approximate) analytical solutions have assumed that the reduced saturation is identically equal to zero at a finite wetting front location, which essentially ignores the structure of the *sharp corner* that appears at the front for large β. In contrast, our asymptotic solution uncovers the detailed structure of the transition within the wetting front, where the solution has very high curvature, and is considerably more accurate that other previous approaches for large β. The asymptotic solution converges polynomially in β and maintains a high degree of accuracy over a wide range of β values corresponding to physical porous media such as soils and rock, unlike many other approaches which are either more limited in their applicability or exhibit a logarithmic singularity near the wetting front as β becomes large. Our approach has the additional advantage that it expresses the solution in terms of explicit formulas instead of requiring numerical approximation of a differential equation (which is required in the approaches of Wagner [9] or Shampine [30]) or inverting the exponential integral function (as in Parlange et al.'s asymptotic solution [18]). In particular, our estimate for y_* may be of value to groundwater researchers and experimentalists since it provides an explicit formula for a measurable quantity (wetting front location) in terms of physical parameter values.

Acknowledgments

This work was funded by grants from the Natural Sciences and Engineering Research Council of Canada, Mitacs Network of Centres of Excellence, Pacific Institute for the Mathematical Sciences, and Engineering and Physical Sciences Research Council.

References

1. W. Brutsaert, Universal constants for scaling the exponential soil water diffusivity?, *Water Resour. Res.* 15:481–483 (1979).
2. B. E. Clothier and I. White, Measurement of sorptivity and soil water diffusivity in the field, *Soil Sci. Soc. Amer. J.* 45:241–245 (1981).
3. R. D. Miller and E. Bresler, A quick method for estimating soil water diffusivity functions, *Soil Sci. Soc. Amer. J.* 41:1020–1022 (1977).
4. K. D. Reichardt, D. R. Nielsen, and J. W. Biggar, Scaling of horizontal infiltration into homogeneous soils, *Soil Sci. Soc. Amer. Proc.* 36:241–245 (1972).
5. W. T. Simpson, Determination and use of moisture diffusion coefficient to characterize drying of northern red oak (*Quercus rubra*), *Wood Sci. Tech.* 27:409–420 (1993).
6. L. Pel, *Moisture transport in porous building materials*, Ph.D. thesis Technische Universiteit Eindhoven (1995).
7. C. Leech, D. Lockington, and P. Dux, Unsaturated diffusivity functions for concrete derived from NMR images, *Matér. Constr.* 36:413–418 (2003).
8. L. Y. Cooper, Constant temperature at the surface of an initially uniform temperature, variable conductivity half space, *J. Heat Transfer* 93:55–60 (1971).
9. C. Wagner, Diffusion of lead chloride in solid silver chloride, *J. Chem. Phys.* 18:1227–1230 (1950).
10. C. M. Hansen, Diffusion in polymers, *Polymer Eng. Sci.* 20:252–258 (1980).
11. G. C. T. Wei and B. J. Wuensch, Tracer concentration gradients for diffusion coefficients exponentially dependent on concentration, *J. Amer. Ceramic Soc.* 59:295–299 (1976).

12. J. L. Vázquez, *The Porous Medium Equation: Mathematical Theory*, *Oxford Mathematical Monographs* Clarendon Press, Oxford, 2007.
13. L. F. Shampine, Concentration-dependent diffusion. II. Singular problems, *Quart. Appl. Math.* 31:287–293 (1973).
14. J. Crank, *The Mathematics of Diffusion*, second ed., Oxford University Press, 1975.
15. J. Parslow, D. Lockington, and J.-Y. Parlange, A new perturbation expansion for horizontal infiltration and sorptivity estimates, *Transp. Porous Media* 3:133–144 (1988).
16. D. K. Babu, Infiltration analysis and perturbation methods. 1. Absorption with exponential diffusivity, *Water Resour. Res.* 12:89–93 (1976).
17. J.-Y. Parlange, A note on a three-parameter soil-water diffusivity function – Application to the horizontal infiltration of water, *Soil Sci. Soc. Amer. J.* 37:318–319 (1973).
18. M. B. Parlange, S. N. Prasad, J.-Y. Parlange, and M. J. M. Römkens, Extension of the Heaslet-Alksne technique to arbitrary soil water diffusivities, *Water Resour. Res.* 28:2793–2797 (1992).
19. C. M. Elliott, M. A. Herrero, J. R. King, and J. R. Ockendon, The mesa problem: Diffusion patterns for $u_t = \nabla \cdot (u^m \nabla u)$ as $m \to +\infty$, *IMA J. Appl. Math.* 37:147–154 (1986).
20. J. R. King, Approximate solutions to a nonlinear diffusion equation, *J. Eng. Math.* 22:53–72 (1988).
21. J. R. King and C. P. Please, Diffusion of dopant in crystalline silicon: An asymptotic analysis, *IMA J. Appl. Math.* 37:185–197 (1986).
22. J. Bear, *Dynamics of Fluids in Porous Media*, Dover, New York, 1988.
23. W. W.-G. Yeh and J. B. Franzini, Moisture movement in a horizontal soil column under the influence of an applied pressure, *J. Geophys. Res.* 71:5151–5157 (1968).
24. P. Amodio, C. J. Budd, O. Koch, G. Settanni, and E. B. Weinmüller, Asymptotical computations for a model of flow in saturated porous media, *Appl. Math. Comput.* 237:155–167 (2014).
25. R. R. Bruce and A. Klute, The measurement of soil moisture diffusivity, *Soil Sci. Soc. Amer. J.* 20:458–462 (1956).
26. J. R. Philip, General method of exact solution of the concentration-dependent diffusion equation, *Aust. J. Phys.* 13:1–12 (1960).
27. J. R. Philip, On solving the unsaturated flow equation: 1. The flux-concentration relation, *Soil Sci.* 116:328–335 (1973).
28. J.-Y. Parlange, Theory of water-movement in soils: 1. One-dimensional absorption, *Soil Sci.* 111:134–137 (1971).
29. M. A. Heaslet and A. Alksne, Diffusion from a fixed surface with a concentration-dependent coefficient, *J. Soc. Ind. Appl. Math.* 9:584–596 (1961).
30. L. F. Shampine, Some singular concentration dependent diffusion problems, *Z. angew. Math. Mech.* 53:421–422 (1973).

Department of Mathematical Sciences, University of Bath, Bath, United Kingdom, BA2 7AY

Department of Mathematics, Simon Fraser University, Burnaby, BC, Canada, V5A 1S6